Magnetotransport through an Aharonov–Bohm ring with parallel double quantum dots coupled to ferromagnetic leads*

Wu Shao-Quan(吴绍全)†, Hou Tao(侯 涛),
Zhao Guo-Ping(赵国平), and Yu Wan-Lun(余万伦)

College of Physics and Electronic Engineering, Sichuan Normal University, Chengdu 610068, *China*

(Received 23 June 2009; revised manuscript received 8 August 2009)

Using the Keldysh nonequilibrium Green function and equation-of-motion technique, this paper studies the magnetotransport through an Aharonov–Bohm (AB) ring with parallel double quantum dots coupled to ferromagnetic leads. It calculates the transmission probability in both the equilibrium and the nonequilibrium case, analyses the conductance and the tunnel magnetoresistance for various parameters, and obtains some new results. These results show that this system is provided with an excellent spin filtering property, and that a large tunnelling magnetoresistance and a negative tunnelling magnetoresistance can arise by adjusting relative parameters; these facts indicate that this system is a possible candidate for spin valve transistors, and has important applications in spintronics.

Keywords: Kondo effect, double quantum dots, Aharonov–Bohm ring, magnetoresistance

PACC: 7225, 7520H, 7320D

1. Introduction

In recent years, the magnetoresistance phenomenon in the semiconductor quantum dot (QD) has attracted great interest as it is the crucial ingredient in the emerging field of spintronics and several quantum computation schemes.[1,2] For example, it makes tunnel transport possible at low temperatures even if the system is in the Coulomb blockage regime, and it offers effective possibilities for the study of strongly correlated electrons because relevant parameters of the QD can be experimentally tuned in a continuous and reproducible manner. When a QD is contacted to two metallic leads, the Kondo effect arises as a result of the coherent superposition of cotunnelling processes, which is now well understood.[3,4] Since the Kondo effect originates from many-body effects due to internal spin degrees of freedom, transport properties are quite sensitive to applied magnetic fields. This fact has naturally stimulated intensive works on spin-polarized transport phenomena for a QD connected to ferromagnetic (FM) leads, giving interesting examples in a rapidly developing field of spintronics. In contrast to the single QD, the double-quantum-dot (DQD) system has attracted much more attention because of their potential industrial applications in device.[5−8] On the one hand, with recent advances in nanofabrication technology, the related experiments can be performed under controlled circumstances, and the DQD system provides an ideal model system for studying the two-impurity effect,[9] which has long been a highlight of condensed-matter physics.[10] On the other hand, the Kondo effect in the DQD system has been observed experimentally, opening prospects for exploring further exotic phenomena due to electron correlations in nanoscale systems.

2. Formulation of the model

In this article, we use the Keldysh nonequilibrium Green function technique to study the magnetotransport through the parallel DQD system connected symmetrically to two FM leads, which is schematically illustrated in Fig. 1. Our model is described by the following Anderson Hamiltonian:

$$H = \sum_{K\alpha\sigma} \varepsilon_{K\alpha\sigma} c^{\dagger}_{K\alpha\sigma} c_{K\alpha\sigma} + \sum_{i\sigma} \varepsilon_{i\sigma} d^{\dagger}_{i\sigma} d_{i\sigma} + U \sum_{i\sigma} n_{i\uparrow} n_{i\downarrow}$$

*Project supported by the Scientific Research Fund of the Education Department of Sichuan Province of China (Grant No. 2006A069) and Funds for Major Basic Research Project of Sichuan Province of China (Grant No. 2006J13-155).
†Corresponding author. E-mail: sqwucd@yahoo.com.cn
© 2010 Chinese Physical Society and IOP Publishing Ltd

$$+\sum_{iK\alpha\sigma}(V_{\alpha i}c^{\dagger}_{K\alpha\sigma}d_{i\sigma}+V^{*}_{\alpha i}d^{\dagger}_{i\sigma}c_{K\alpha\sigma}), \quad (1)$$

where $c^{\dagger}_{K\alpha\sigma}(c_{K\alpha\sigma})$ is the creation (annihilation) operator of an electron with energy $\varepsilon_{K\alpha\sigma}$ and spin σ in the lead α (α=L, R), and $d^{\dagger}_{i\sigma}(d_{i\sigma})$ represents the creation (annihilation) operator of an electron for dot i ($i=1,2$) at the impurity site. The last term denotes the coupling between the leads and the two dots, the parameter $V_{\alpha i}$ describes the hopping amplitude from the α electrode to the QD$_i$; we choose a system gauge such as $(V_{\rm L1})^{*}=V_{\rm L2}=(V_{\rm R2})^{*}=V_{\rm R1}=|V|\exp(\mathrm{i}\,\varphi/4)$ and $\varphi=2\pi\Phi/\Phi_0$ with Φ and $\Phi_0=hc/e$ being the magnetic flux and the flux quantum, respectively.

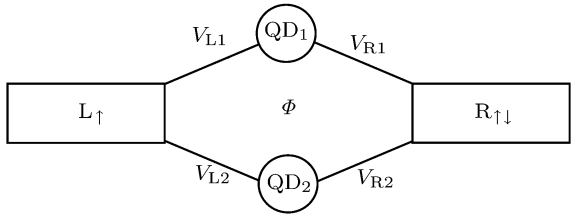


Fig. 1. Schematic picture of the parallel DQD system coupled to the FM leads. Where $V_{\alpha i}$ (α=L, R, i=1, 2) describes the hopping amplitude from the α electrode to the QD$_i$ ($i=1,2$) and Φ represents the magnetic flux.

The current from the left electrode can be calculated from the time evolution of the occupation number operator of the left electrode:

$$\begin{aligned}I_{\rm L}(t)&=-e\langle\dot{N}_{\rm L}\rangle=-\frac{\mathrm{i}\,e}{\hbar}\langle[H,N_{\rm L}]\rangle\\&=\frac{\mathrm{i}\,e}{\hbar}\sum_{\mathrm{i}\,k\sigma}(V_{{\rm L}i}\langle c^{\dagger}_{k{\rm L},\sigma}d_{i\sigma}\rangle-V^{*}_{{\rm L}i}\langle d^{\dagger}_{i\sigma}c_{k{\rm L},\sigma}\rangle).\end{aligned} \quad (2)$$

Using the Keldysh nonequilibrium Green function formalism and Ng's ansatz: $G^{<}_{\sigma}=G^{\rm a}_{\sigma}\Sigma^{<}G^{\rm r}_{\sigma}$ and $\Sigma^{<}=\Sigma^{<}_{0}(\Sigma^{\rm r}_{0}-\Sigma^{\rm a}_{0})^{-1}(\Sigma^{\rm r}-\Sigma^{\rm a})$,[11] we can write the current in a Landauer–Büttiker form in terms of the Green function of DQD

$$I_{\rm L}=\frac{e}{h}\int{\rm d}\omega\sum_{\sigma}T_{\sigma}(\omega)(f_{\rm L}(\omega)-f_{\rm R}(\omega)), \quad (3)$$

where $f_{\alpha}(\omega)=(\mathrm{e}^{\beta(\omega-\mu_{\alpha})}+1)^{-1}$ is the Fermi distribution function of lead α with the different chemical potential upon a voltage bias $\mu_{\rm L}-\mu_{\rm R}=eV$, and the total transmission probability $T_{\sigma}(\omega)$ per spin is given by

$$T_{\sigma}(\omega)={\rm Tr}[\Gamma^{\rm L}_{\sigma}G^{\rm r}_{\sigma}\bar{\Sigma}^{<}G^{\rm a}_{\sigma}]. \quad (4)$$

Defining $\bar{\Sigma}^{<}=\Gamma^{\rm R}_{\sigma}(\Gamma^{\rm L}_{\sigma}+\Gamma^{\rm R}_{\sigma})^{-1}(\Sigma^{\rm R}_{\sigma}-\Sigma^{\rm a}_{\sigma})$, we get that

$$\Gamma^{\rm L}_{\sigma}=\frac{1}{2}\begin{bmatrix}\Gamma^{\rm L}_{1\sigma} & \mathrm{e}^{\mathrm{i}\,\varphi/2}\Gamma^{\rm L}_{12\sigma}\\ \mathrm{e}^{-\mathrm{i}\,\varphi/2}\Gamma^{\rm L}_{21\sigma} & \Gamma^{\rm L}_{2\sigma}\end{bmatrix},$$

and

$$\Gamma^{\rm R}_{\sigma}=\frac{1}{2}\begin{bmatrix}\Gamma^{\rm R}_{1\sigma} & \mathrm{e}^{-\mathrm{i}\,\varphi/2}\Gamma^{\rm R}_{12\sigma}\\ \mathrm{e}^{\mathrm{i}\,\varphi/2}\Gamma^{\rm R}_{21\sigma} & \Gamma^{\rm R}_{2\sigma}\end{bmatrix} \quad (5)$$

are line width matrices with $\Gamma^{\alpha}_{ij\sigma}(\omega)=2\pi\sum_{k}V^{*}_{\alpha i}V_{\alpha j}\delta(\omega-\varepsilon_{k\alpha\sigma})$. In order to determine the retarded Green function (GF), we choose the equation-of-motion method.[12] The retarded/advanced (GF) $G^{\rm r/a}_{\sigma}(\omega)$ has 2×2 matrix structure, which accounts for the DQD structure of the system, and in the limit $U\to\infty$, it is determined explicitly to read as:

$$G^{\rm r}_{\sigma}(\omega)=\begin{pmatrix}G^{\rm r}_{11\sigma} & G^{\rm r}_{12\sigma}\\ G^{\rm r}_{21\sigma} & G^{\rm r}_{22\sigma}\end{pmatrix}=\frac{1}{a_{1\sigma}a_{2\sigma}-d_{1\sigma}d_{2\sigma}}\begin{pmatrix}a_{2\sigma}\,(1-\langle n_{1\bar{\sigma}}\rangle) & -d_{1\sigma}\,(1-\langle n_{2\bar{\sigma}}\rangle)\\ -d_{2\sigma}\,(1-\langle n_{1\bar{\sigma}}\rangle) & a_{1\sigma}\,(1-\langle n_{2\bar{\sigma}}\rangle)\end{pmatrix}. \quad (6)$$

The advanced GF is given by $G^{\rm a}_{\sigma}(\omega)=[G^{\rm r}_{\sigma}(\omega)]^{+}$. Here

$$\begin{aligned}a_{1\sigma}&=\omega-\varepsilon_{1\sigma}-\Big(-\frac{\mathrm{i}}{2}(\Gamma^{\rm L}_{1\sigma}+\Gamma^{\rm R}_{1\sigma})\Big)-\Sigma^{\rm r}_{1\sigma}(\omega),\\ a_{2\sigma}&=\omega-\varepsilon_{2\sigma}-\Big(-\frac{\mathrm{i}}{2}(\Gamma^{\rm L}_{2\sigma}+\Gamma^{\rm R}_{2\sigma})\Big)-\Sigma^{\rm r}_{2\sigma}(\omega),\\ d_{1\sigma}&=\frac{\mathrm{i}}{2}(\mathrm{e}^{\mathrm{i}\,\varphi/2}\sqrt{\Gamma^{\rm L}_{1\sigma}\Gamma^{\rm L}_{2\sigma}}+\mathrm{e}^{-\mathrm{i}\,\varphi/2}\sqrt{\Gamma^{\rm R}_{1\sigma}\Gamma^{\rm R}_{2\sigma}}),\end{aligned}$$

and

$$d_{2\sigma}=\frac{\mathrm{i}}{2}(\mathrm{e}^{-\mathrm{i}\,\varphi/2}\sqrt{\Gamma^{\rm L}_{1\sigma}\Gamma^{\rm L}_{2\sigma}}+\mathrm{e}^{\mathrm{i}\,\varphi/2}\sqrt{\Gamma^{\rm R}_{1\sigma}\Gamma^{\rm R}_{2\sigma}})$$

with

$$\Sigma^{\rm r}_{1\sigma}(\omega)=\sum_{k\alpha}\frac{|V_{k1}|^{2}\,f_{\rm L/R}(\varepsilon_{k\bar{\sigma}})}{\omega-\tilde{\varepsilon}_{1\sigma}+\tilde{\varepsilon}_{1\bar{\sigma}}-\varepsilon_{k\alpha\bar{\sigma}}+\mathrm{i}\,0^{+}}$$

and

$$\Sigma^{\rm r}_{2\sigma}(\omega)=\sum_{k\alpha}\frac{|V_{k2}|^{2}\,f_{\rm L/R}(\varepsilon_{k\bar{\sigma}})}{\omega-\tilde{\varepsilon}_{2\sigma}+\tilde{\varepsilon}_{2\bar{\sigma}}-\varepsilon_{k\alpha\bar{\sigma}}+\mathrm{i}\,0^{+}},$$

where $\tilde{\varepsilon}_{i\sigma}$ represents the renormalised spin levels, which is found to satisfy the self-consistent equation $\tilde{\varepsilon}_{i\sigma}=\varepsilon_{i\sigma}+{\rm Re}\,\Sigma^{\rm r}_{i\sigma}(\tilde{\varepsilon}_{i\sigma},\tilde{\varepsilon}_{i\bar{\sigma}})$.[13] The occupation num-

ber operator of the QD$_i$ with spin σ is given by

$$\langle n_{i\sigma}\rangle = -\frac{\mathrm{i}}{2\pi}\int \mathrm{d}\omega \mathrm{Im}G^{<}_{ii\sigma}(\omega),$$

and the density of states (DOS) in the QD$_i$ is $\rho_{i\sigma}(\omega) = -(1/\pi)\mathrm{Im}G^{\mathrm{r}}_{ii\sigma}(\omega)$.

We consider two magnetic configurations, namely, parallel (P) and antiparallel (AP) configurations. When the magnetic electrodes are in P configuration, we assume that the spin-majority electrons are up ($\uparrow$) and the spin-minority electrons are down ($\downarrow$). We further assume that in the AP configuration the magnetization of the right electrode is reversed, and we introduce the effective spin-polarization strength p_α, which is defined as $p_\alpha = \Gamma^\alpha_\sigma - \Gamma^\alpha_{\bar\sigma}/\Gamma^\alpha_\sigma + \Gamma^\alpha_{\bar\sigma}$ $(0 \le p_\alpha \le 1)$. Therefore the spin dependence of the coherent transport can be conveniently considered by introducing magnetic polarization factors p_{L} and p_{R} for the left and right leads, respectively. From the definition of p_α, Γ^α_σ can be expressed as $\Gamma^{\mathrm{L}}_{\uparrow(\downarrow)} = \Gamma_0(1 \pm p_{\mathrm{L}}), \Gamma^{\mathrm{R}}_{\uparrow(\downarrow)} = \Gamma_0(1 \pm p_{\mathrm{R}})$ for the P configuration and $\Gamma^{\mathrm{L}}_{\uparrow(\downarrow)} = \Gamma_0(1 \pm p_{\mathrm{R}})$, $\Gamma^{\mathrm{R}}_{\uparrow(\downarrow)} = \Gamma_0(1 \mp p_{\mathrm{R}})$ for the AP configuration, where Γ_0 describes the coupling between the QD and electrodes without internal magnetization and is used as the unit of energy. In this work, we adopt the symmetric leads, i.e. $p_{\mathrm{L}} = p_{\mathrm{R}} = p$.

For simplicity, the temperature is taken as $T = 0.005\Gamma_0$, the energy level of the two dots is fixed at $\varepsilon_{1\sigma} = \varepsilon_{2\sigma} = -4.0\Gamma_0$, and the conduction band has a constant DOS with the bandwidth $D = 100\Gamma_0$.

3. Results

In Fig. 2, we plot the transmission probability for up-spin and down-spin electrons of the two dots for various spin-polarized strength p in the P and AP configurations when the magnetic flux φ is equal to 0.0 and $\pi/2$. From all the figures, we can see that there is a sharp peak around the Fermi energy which is caused by the Kondo effect. It is seen that in the P configuration, the contribution of up-spin (i.e. majority spin) electrons is dramatically different from that of down-spin (i.e. minority spin) electrons. We can also see that with the increase of p, the peak in the Fermi level moves in the opposite directions for different spins. For up-spin electrons, it moves left, while it moves right for down-spin electrons. Furthermore, the amplitude of the transmission probability for up-spin electrons increases as p increases (Figs. 2(a) and 2(b)). In contrast, with the increase of p, the peaks of the transmission probability for down-spin electrons decrease greatly with the increase of p (Figs. 2(e) and 2(f)). Therefore, the total transmission probability mainly comes from the contribution of up-spin electrons.

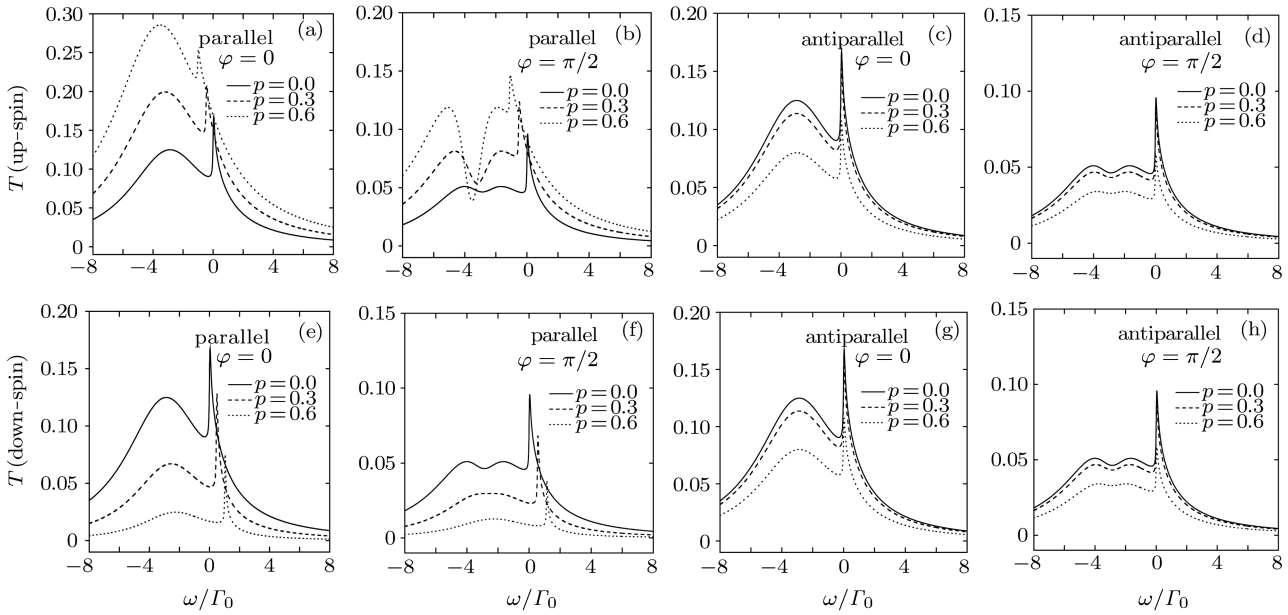


Fig. 2. The transmission probability of the two dots with both P and AP lead-polarization alignments as a function of the energy level for spin-up and spin-down configurations, calculated for various values of the magnetic flux φ and spin-polarization strength p in the equilibrium case.

This happens because in the P configuration and $p \neq 0$, there is an overall asymmetry for up- and down-spins, namely, $\rho_{L\uparrow} + \rho_{R\uparrow} > \rho_{L\downarrow} + \rho_{R\downarrow}$, so the hybridization for up-spins is larger than that for down-spins ($\Gamma_{\alpha\uparrow} > \Gamma_{\alpha\downarrow}$) because of the spin-dependent DOS in leads. Additionally, the bare level $\varepsilon_{i\sigma}$ is renormalized and the up-spin (down-spin) electron lowers (raises) its energy. Thus, the average occupation of the QD with up-spins is larger than that with down-spins ($n_{d\uparrow} > n_{d\downarrow}$). All these enhance the transmission probability of up-spin electrons through this system, while the down-spin electron transport through this system is suppressed. In the AP configuration, a remarkable point is that the behaviour of the transmission probability for up- (Figs. 2(c) and 2(d)) and down-spins (Figs. 2(g) and 2(h)) in leads is identical, which also has only one sharp peak at the Fermi energy for different values of p. In this situation, the DOS for up- and down-spins in leads are the same, $\rho_{L\uparrow}+\rho_{R\uparrow} = \rho_{L\downarrow}+\rho_{R\downarrow}$, and the spin current of electrons cannot be polarized. In other words, under the condition of AP configuration, electrode effects on electrons in QDs fully counteract. Therefore, in addition to the influence of the spin-polarization strength, the rate of each spin (up-spin and down-spin) in the QD is the same, resulting in zero net magnetic moment of the QD. This moment (i.e. the Kondo resonance) forms, which is the same as those for non-magnetic electrodes, and up-spin electrons make the same contribution to the transmission probability as down-spin electrons behave. Moreover, it is interesting to note that the amplitude of the transmission probability decreases with the increase of the spin-polarization strength p, because the magnetization of electrodes suppresses the Kondo resonance in this system.

In order to clearly observe the characteristic p-dependence in the transmission probability, let us consider the contribution of up- and down-spin electrons in both P and AP lead-polarization alignment to $T(\varepsilon)$ in the nonequilibrium case, too. When the bias voltage is applied, the Fermi levels of the two electrodes are different. We wish to study the transport properties for FM leads with finite bias voltage, here we set the chemical potentials $\mu_L = 0.2$, $\mu_R = -0.2$. In Fig. 3, the transmission probability of the two dots in the nonequilibrium case is presented. As observed from Fig. 3, we can easily find that the overall behaviour of the transmission probability here is similar to that in the equilibrium case (Fig. 2), but the origin of the characteristics is somewhat different. The Kondo peak is always located at energies coinciding with those of the Fermi levels of the leads, which is now well understood. Thus in the nonequilibrium case, we can obtain two Kondo resonances pinned to Fermi energies of the left and right electrodes.

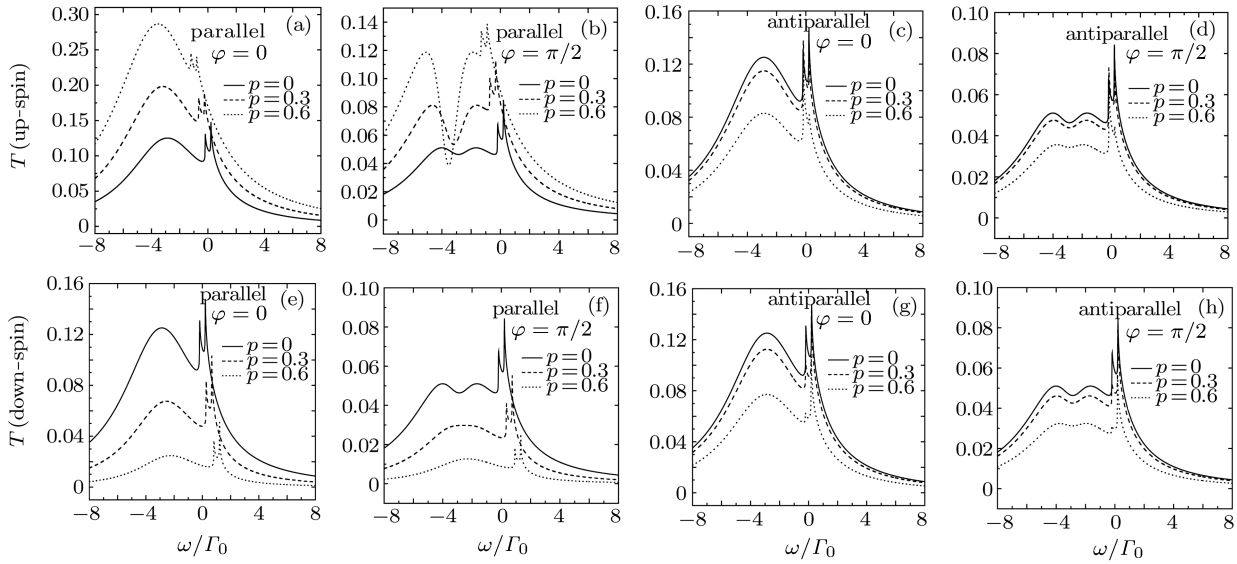


Fig. 3. The transmission probability of the two dots with both P and AP lead-polarization alignments as a function of the energy level for spin-up and spin-down configurations, calculated for various values of φ and spin-polarization strength p in the nonequilibrium.

From Fig. 3, we can easily see that when the chemical potentials split, the Kondo peak at the Fermi level also splits, giving rise to two suppressed Kondo peaks in the vicinity of the Fermi energy of the electrodes. In other words, when the bias voltage is applied, the Kondo peak splits into two located peaks at the chemical potentials with lower intensities. This originates from the cotunnelling processes of the electrons between the left and right leads. Additionally, we can also obtain that the splitting of the Kondo peak is equal to eV ($\mu_{\rm L} - \mu_{\rm R} = eV$), which is in good agreement with that in Ref. [14].

To further describe the magnetoresistance phenomenon of this system, we plot the variation of the linear conductance $G_{V=0}$ and the tunnelling magnetoresistance (TMR) with the dot's level position ε_d for different magnetic flux in Fig. 4. The TMR of the system is defined by TMR $= (G^{\rm P}\big|_{V=0} - G^{\rm AP}\big|_{V=0})/\, G^{\rm AP}\big|_{V=0}$, where $G^{\rm P}\big|_{V=0}$ and $G^{\rm AP}\big|_{V=0}$ are the linear conductance for P and AP configurations, respectively. In Fig. 4, one can see the crossover behaviour of the linear conductance and the TMR from $\varphi = 0.0$ to $\varphi = \pi/2.0$. When the dot's level ε_d is far from resonance ($|\varepsilon_d| \gg 0$), the linear conductance $G_{V=0}$ decreases with the increase of $|\varepsilon_d|$ due to the suppression of charge fluctuations in the DQD, while the TMR is nearly independent of the dot's level ε_d, coinciding with the noninteracting case. This situation changes when this system goes into the mixed-valence regime. At this moment, the TMR is very sensitive to the dot's level ε_d because of the presence of large charge fluctuations. Especially when $\varphi \neq 0$, the linear conductance splits into two peaks coming from the interference between resonant transport through two single levels, and the TMR develops into a dip with a negative value. In the empty orbital regime where the dot level is higher than the chemical potential of the electrodes, the TMR may be enhanced to a value as large as 250% when $\varphi = \pi/2.0$. The presence of the large TMR and the negative TMR indicates that this system is provided with an excellent spin filtering property, and this property has important applications in spintronics.

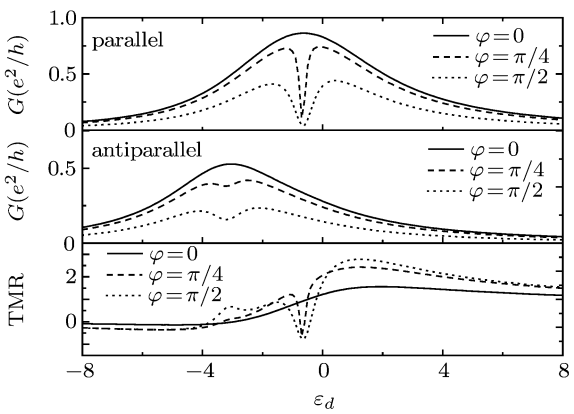


Fig. 4. Linear conductance $G_{V=0}$ and tunnelling magnetoresistance TMR as a function of the level position ε_d with $p = 0.5$. The other model parameters are the same as those in Fig. 2.

In Fig. 5, we plot the TMR as a function of AB phase φ for several values of ε_d. One can see that at $\varepsilon_d = -4$ (Kondo regime) and $\varepsilon_d = 4$ (empty orbital regime), the TMR exhibits peak valences at $\varphi = \pi$ and $\varphi = 3\pi$ due to the presence of difference constructive and destructive interference between resonant transports through two single levels. At this moment, there is the global phase difference of $\phi + \delta_{d\sigma}$ between electrons transmitted through two channels, so the functional form of the TMR exhibits a sine line shape, which is similar to magnetic tunnel junctions. But on the other hand, there is a larger charge fluctuation in the empty orbital regime than that in the Kondo regime, which leads to much larger peak valences of the TMR in the empty orbital regime than those in the Kondo regime. The situation changes when the system goes into the mixed-valence regime ($\varepsilon_d = 0$). In this instant, there are both large charge fluctuations and the electron interaction in the DQD, thus the peak valences occur at $\varphi = 0$, $\varphi = 2\pi$ and $\varphi = 4\pi$, which lead to the different line shapes of the TMR as a function of the magnetic flux φ.

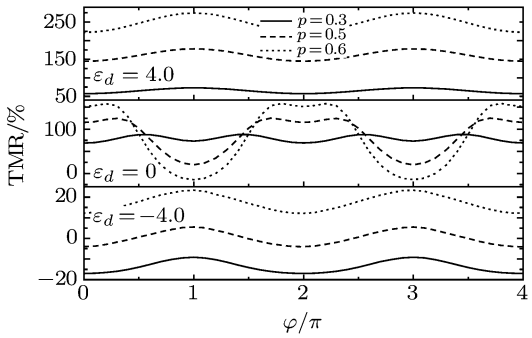


Fig. 5. The TMR as a function of the magnetic flux φ for various values of the level position ε_d and spin-polarization strength p. The model parameters are the same as those in Fig. 2.

4. Conclusions

In conclusion, using the Keldysh nonequilibrium Green function technique, we have presented a qualitative study of the transport properties of an

Aharonov–Bohm ring with parallel DQDs coupled to two ferromagnetic leads. Our results show that transport properties of nonequilibrium are different from those of the equilibrium case, and there are two transmission peaks in the nonequilibrium due to Kondo effect, one for each chemical potential. Moreover, we also find that this system is sensitive to the spin polarization of the electrode and the magnetic flux. For the P configuration, the transmission probability is mainly contributed by up-spin electrons, but for the AP configuration, the contributions of the up- and down-spin electrons are always the same. On the other hand, the conductance is sensitive to the spin polarization of the electrode and the magnetic flux, and a large TMR and a negative TMR can arise by adjusting relative parameters. The rich physical behaviour of this system may have potential applications in spintronics, and this system might be a possible candidate for spin-filter devices. We hope that this work will encourage further efforts, both theoretical and experimental, to probe both the equilibrium and nonequilibrium physics of interacting quantum systems.

References

[1] Prinz G A 1998 *Science* **282** 1660
Wolf S A and Treger D M 2001 *Science* **294** 1488

[2] Lu R and Liu Z R 2002 cond-mat/0210350
Yan C H, Wu S Q, Huang R and Sun W L 2008 *Chin. Phys.* B **17** 296
Yang F B, Wu S Q, Yan C H, Huang R, Hou T and Sun W L 2008 *Chin. Phys.* B **17** 1383

[3] Hewson A C 1993 *The Kondo Problem to Heavy Fermions* (Cambridge: Cambridge University Press)
Goldhaber-Gordon D, Shtrikman H, Mahalu D, Abusch Magder D, Meirav U and Kastner M A 1998 *Nature* **391** 156
Cronenwett S M, Oosterkamp T H and Kouwenhoven L P 1998 *Science* **281** 540

[4] Sun Q F, Guo H and Lin T H 2001 *Phys. Rev. Lett.* **87** 176601
Kouwenhoven L P and Glazman L 2001 *Phys. World* **14** 33

[5] Georges A and Meir Y 1999 *Phys. Rev. Lett.* **82** 3508
Aguado R and Langreth D C 2000 *Phys. Rev. Lett.* **85** 1946

[6] Wu S Q, Wang S J, Sun W L and Yu W L 2004 *Chin. Phys.* **13** 510
Wu S Q, He Z, Yan C H, Chen X W and Sun W L 2006 *Acta Phys. Sin.* **55** 1413 (in Chinese)
Wu S Q, Sun W L, Yu W L and Wang S J 2005 *Acta Phys. Sin.* **54** 2910 (in Chinese)
Zhou B, Wu S Q, Sun W L and Zhou X L 2004 *Chin. Phys.* **13** 225

[7] Yoffe A D 2001 *Adv. Phys.* **50** 1
Loss D and Divincenzo D P 1998 *Phys. Rev.* A **57** 120
Chen M L and Wang S J 2007 *Chin. Phys.* **16** 2101

[8] Song H Z, Zhang P, Duan S Q and Zhao X G 2006 *Chin. Phys.* **15** 2130
Björn K and Jürgen K 2002 *Phys. Rev.* B **65** 245301
Boese D, Hofstetter W and Schoeller H 2002 *Phys. Rev.* B **66** 125315

[9] Izumida W and Sakai O 2000 *Phys. Rev.* B **62** 10260
Deng Y X, Yan X H and Tang N S 2006 *Acta Phys. Sin.* **55** 2027 (in Chinese)

[10] Jones B A, Varma C M and Wilkins J W 1998 *Phys. Rev. Lett.* **61** 125

[11] Ng T K 1996 *Phys. Rev. Lett.* **76** 487
Zhang P, Xue Q K, Wang Y P and Xie X C 2002 *Phys. Rev. Lett.* **89** 286803

[12] Meir Y and Wingreen N S 1992 *Phys. Rev. Lett.* **68** 2512
Jauho A P, Wingreen N S and Meir Y 1994 *Phys. Rev.* B **50** 5528

[13] Martinek J, Utsumi Y, Imamura H, Barnas J, Maekawa S, König J and Schön G 2003 *Phys. Rev. Lett.* **91** 127203
Sergueev, Sun Q F, Guo H, Wang B G and Wang J 2002 *Phys. Rev.* B **65** 165303
Wang J M, Wang R and Liang J Q 2007 *Chin. Phys.* **16** 2075

[14] Świrkowicz R, Barnaś J and Wilczyński M 2003 *Phys. Rev.* B **68** 195318